Acta Crystallographica Section D
Biological Crystallography
ISSN 0907-4449

Reproducible improvements in order and diffraction limit of crystals of bovine F_1-ATPase by controlled dehydration

Matthew W. Bowler,[a] Martin G. Montgomery,[a] Andrew G. W. Leslie[b]* and John E. Walker[a]*

[a]The Medical Research Council Dunn Human Nutrition Unit, Cambridge, England, and [b]The Medical Research Council Laboratory of Molecular Biology, Cambridge, England

Correspondence e-mail: andrew@mrc-lmb.cam.ac.uk, walker@mrc-dunn.cam.ac.uk

Received 25 April 2006
Accepted 1 June 2006

Orthorhombic crystals of bovine F_1-ATPase have been subjected to controlled dehydration. A decrease in the relative humidity surrounding the crystals to 90% reproducibly reduced their unit-cell volume by 22% (950 000 Å^3) and improved the diffraction limit and mosaic spread of the crystals significantly. These dehydrated crystals diffracted X-rays to 1.8 Å resolution at a synchrotron source, the best diffraction limit yet attained with these crystals, although radiation damage limited the resolution of a complete data set to 1.95 Å.

1. Introduction

ATP synthase (F_1F_o-ATPase) is a large membrane-bound multisubunit complex that catalyses the synthesis of ATP from ADP and orthophosphate using a transmembrane proton motive force generated by respiration or photosynthesis as a source of energy (Walker, 1998). Catalysis takes place in its hydrophilic F_1 domain, which can be purified intact from the complex with retention of its ATP hydrolase activity and crystallized. The structure of the F_1-ATPase from bovine mitochondria has been solved to 2.8 Å resolution (Abrahams *et al.*, 1994) and the structures of several inhibited complexes have been described subsequently (Gibbons *et al.*, 2000; Kagawa *et al.*, 2004; Menz *et al.*, 2001; Orriss *et al.*, 1998; van Raaij *et al.*, 1996). The structure of the enzyme inhibited by ADP and aluminium fluoride, representing a transition-state complex, was determined at 2 Å and is the highest resolution structure of F_1-ATPase described to date (Menz *et al.*, 2001). The unit cell of the crystals used to solve this structure had a significantly smaller *a* parameter (a = 268 Å) relative to crystals of the enzyme in ground-state complexes, where *a* is usually ∼284 Å. In crystals of the complex covalently inhibited by reaction with dicyclohexylcarbodiimide (Gibbons *et al.*, 2000), the *a* parameter of the unit cell was reduced also to ∼267 Å. This shrinkage resulted in new lattice contacts involving the foot of the central stalk, which protrudes about 45 Å from the main spherical body of the complex. This led to a marked improvement in the electron-density map in this region.

Previously, dehydration has been observed to lead to better ordered protein crystals (Cramer *et al.*, 2000; Heras *et al.*, 2003 and references therein) and in some cases the original observation arose accidentally (Esnouf *et al.*, 1998; Kuo *et al.*, 2003). However, until the recent advent of the Free Mounting System (FMS; Kiefersauer *et al.*, 1996, 2000), it has not been possible to dehydrate crystals and to monitor the effect of dehydration on their diffraction properties in a systematic way. The diffraction properties of several protein crystals have been

improved with the FMS (Dobbek *et al.*, 1999; Engel *et al.*, 2003; Estebanez-Perpina *et al.*, 2000; Henrich *et al.*, 2003; Koch *et al.*, 2004; Kyrieleis *et al.*, 2005). As described below, the relative humidity surrounding individual crystals of bovine mitochondrial F_1-ATPase has been changed systematically using an FMS. The effects of dehydration on the diffraction properties of the crystals have been monitored during the dehydration process and conditions for reproducible improvement of diffraction properties have been established. Thus, diffraction has been observed to a maximum of 1.8 Å resolution and a data set has been processed to 1.95 Å. This has allowed a much more accurate ground-state structure to be determined than has been possible hitherto and the binding site of azide, a known inhibitor, has been resolved (Bowler *et al.*, 2006).

2. Materials and methods

2.1. Crystallization

An ammonium sulfate precipitate of purified bovine mitochondrial F_1-ATPase was redissolved in minimal buffer. Crystals of F_1-ATPase were grown in microdialysis buttons (50 µl) with SpectraPor dialysis membranes (3500 Da molecular-weight cutoff). An equal volume of inside buffer [100 m*M* Tris–HCl pH 7.2, 400 m*M* NaCl, 4 m*M* $MgCl_2$, 2 m*M* AMP-PNP, 40 µ*M* ADP, 0.04%(*w*/*v*) NaN_3, 0.004%(*w*/*v*) phenylmethylsulfonyl fluoride and 14%(*w*/*v*) polyethylene glycol 6000 in D_2O] was added slowly to the protein and the solution mixed gently (final concentration 5 mg ml^{-1}). The samples were dialysed against 3 ml outside buffer [50 m*M* Tris–HCl pH 8.2, 200 m*M* NaCl, 20 m*M* $MgSO_4$, 250 µ*M* AMP-PNP, 5 µ*M* ADP, 0.02%(*w*/*v*) NaN_3, 0.004%(*w*/*v*) phenylmethylsulfonyl fluoride and 9%(*w*/*v*) polyethylene glycol 6000]. After 48 h, this buffer was replaced with the same buffer but containing polyethylene glycol 6000 with a range of concentrations (in different vials) from 10 to 12.5%(*w*/*v*) in 0.25% steps. The crystals were fully grown after four weeks. Crystals were grown also from desalted protein in microbatch plates (Nunc Nalgene International). The drops contained a solution (2 µl) consisting of 50 m*M* Tris–HCl pH 8.0, 200 m*M* NaCl, 20 m*M* $MgSO_4$, 0.02%(*w*/*v*) NaN_3, 0.004%(*w*/*v*) phenylmethylsulfonyl fluoride, 1 m*M* ATP and 9–12%(*w*/*v*) polyethylene glycol 6000 in D_2O and an equal volume of protein (final volume 4 µl, final protein concentration 5 mg ml^{-1}). The use of D_2O rather than H_2O resulted in improved diffraction in some previous crystals of bovine F_1-ATPase. Drops were covered with filtered liquid paraffin and kept at room temperature. Crystals were fully grown after one week.

2.2. Crystal dehydration

Crystals were harvested in a LithoLoop (Molecular Dimensions Ltd, Soham, England) or in MicroMesh loops (MiteGen, Ithica, NY, USA) and mounted in a Free Mounting System (FMS; Proteros Biostructures GmbH, Martinsried, Germany) where the relative humidity had been set to match that of the mother liquor (in this case 99%) by the loop method (Kiefersauer *et al.*, 1996). Briefly, a loop containing a drop of mother liquor was placed in the FMS head and its volume was monitored. Then the relative humidity was adjusted until the volume of the drop remained constant, at which point the equivalent humidity to the mother liquor is known. Crystals were picked up in loops and mounted on the FMS head. Excess mother liquor was removed from the

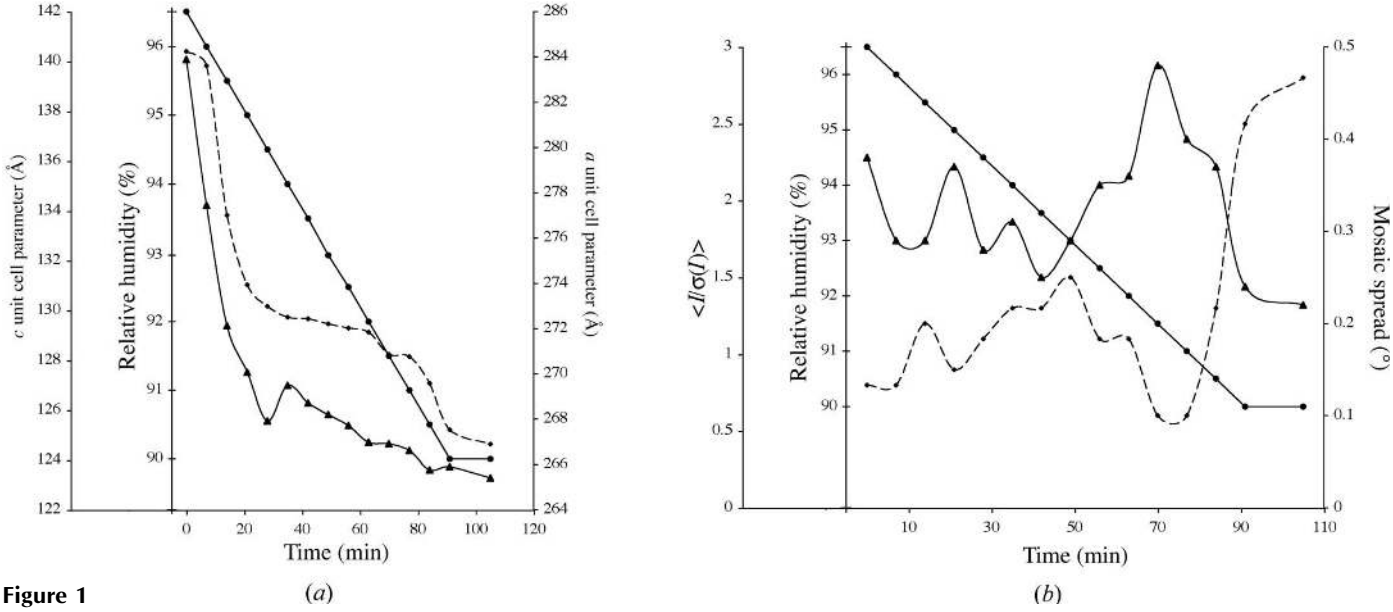

Figure 1
Influence of controlled dehydration on (*a*) the unit-cell parameters and (*b*) mosaic spread and $\langle I/\sigma(I)\rangle$ of a crystal of bovine F_1-ATPase. The crystal orientation was fixed and still diffraction patterns were recorded every 5 min, corresponding to a decrease in relative humidity of 0.5%. (*a*) The changes in the *a* and *c* unit-cell parameters with relative humidity are plotted as solid and dotted lines, respectively. The relative humidity is plotted as filled circles. The *b* unit-cell parameter decreases by less than 1 Å during dehydration. (*b*) The change in the mosaic spread and $\langle I/\sigma(I)\rangle$ for the outer shell (4.75–4.44 Å) are plotted as solid and dotted lines, respectively. The relative humidity is plotted as filled circles.

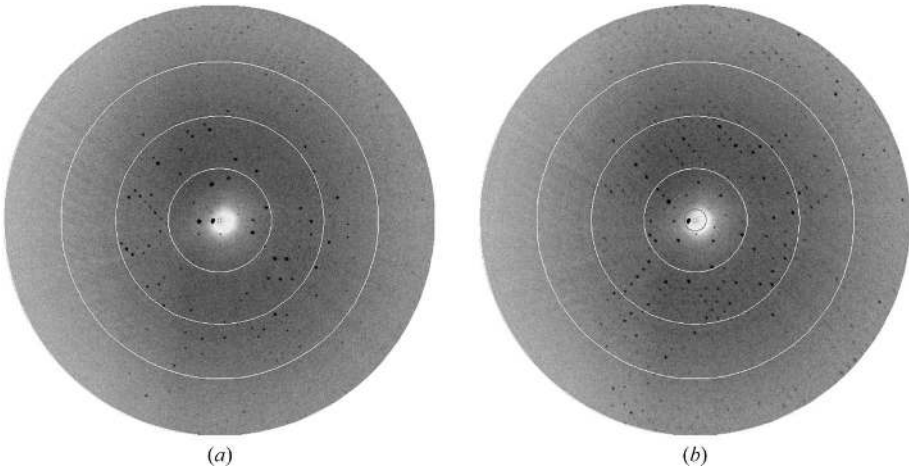

Figure 2
Improvement in diffraction limit during dehydration of a crystal of F_1-ATPase. The circles mark the 14.7, 7.3, 4.9 and 3.7 Å resolution shells. The unit-cell parameters for (*a*) were $a = 284.36$, $b = 108.2$, $c = 141.68$ Å. The unit-cell parameters for (*b*) were $a = 264.2$, $b = 107.4$, $c = 124.04$ Å. The images were taken between a relative humidity of 98% (*a*) and 90% (*b*). The shadow is caused by the head of the FMS.

crystal. A still diffraction image obtained with Cu $K\alpha$ X-radiation from a Rigaku H3R generator was recorded with a MAR 345 image-plate detector. Then the relative humidity was reduced in a gradient from 99 to 85% (at 0.1% min^{-1}) and diffraction images were recorded continuously at room temperature with an exposure time of 5 min (corresponding to an 0.5% decrease in relative humidity). The diffraction limit, unit-cell parameters and mosaic spread were determined for each image with *MOSFLM* (Leslie, 1992). The humidity required to give maximally diffracting crystals was determined and crystals were maintained at this humidity for several minutes to allow complete equilibration. A final image was recorded to monitor any further changes to the crystal and the crystals were then cryocooled by plunging into liquid nitrogen either directly or after coating them in a thin film of perfluoropolyether oil (Alfa Aeasar, Heysham, England). Crystals were examined on beamline ID14-4 at the European Synchrotron Radiation Facility, Grenoble, France.

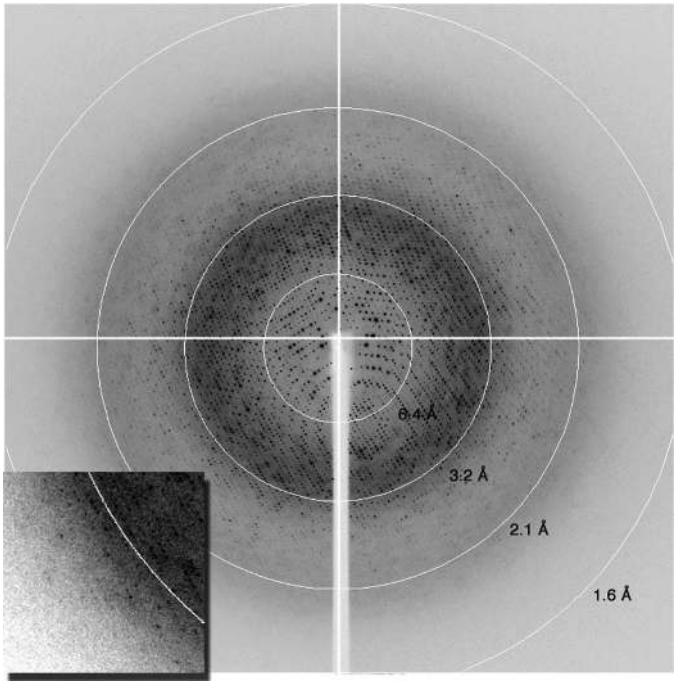

Figure 3
Diffraction of a dehydrated crystal (X1) of F_1-ATPase at a synchrotron source. Circles mark resolution shells. Diffraction was observed to a limit of 1.8 Å (inset, where the arc of the circle is at 2.1 Å resolution).

3. Results and discussion

3.1. Effect of dehydration on crystals

Bovine mitochondrial F_1-ATPase crystallizes in an orthorhombic space group, $P2_12_12_1$, with typical unit-cell parameters of $a = 284$, $b = 108$, $c = 140$ Å, although a range of values have been observed in cryocooled crystals, especially for the *a* parameter. In the current experiments, the crystals of bovine F_1-ATPase were mounted in the FMS at a relative humidity of 99%. Their unit-cell parameters and mosaic spread were similar to capillary-mounted crystals (Lutter *et al.*, 1993). When the relative humidity was reduced, the unit-cell parameters decreased and the diffraction limit improved (Figs. 1 and 2). It is noteworthy that the diffraction properties of the crystal continue to improve after the relative humidity reaches its lower limit of 90%. This reflects the time taken for the crystal to equilibrate fully in the moist air stream, which will probably depend on crystal size (this was not investigated further). The crystal used in this experiment had dimensions of $0.5 \times 0.3 \times 0.4$ mm. During dehydration, the crystals went through two main transformations. Initially, between 98 and 93.5% relative humidity, the crystal quality improved with a concomitant reduction in the *a* and *c* parameters of ~10 Å. From 93.5 to 91.5% relative humidity, the crystals first deteriorated (Fig. 1*b*) and then improved again (a series of diffraction patterns recorded during this part of the dehydration process are presented as a movie in the supplementary material[1]). The best diffraction was observed at a relative humidity of 90%. When the relative humidity was reduced below 90% the diffraction deteriorated and below 87% the deterioration was both rapid and irreversible.

There was also some variability between crystals and their reaction to dehydration. Crystals grown by microbatch rather than microdialysis appeared to be more sensitive to changes in relative humidity. A relative humidity of <97% destroyed crystal order, probably because the crystals were dehydrated partially during growth (as suggested by the unit-cell parameters) by water loss into the oil phase. Some of these crystals

[1] Supplementary material has been deposited in the IUCr electronic archive (Reference: HV5059). Services for accessing this material are described at the back of the journal.

Table 1
Data-processing statistics.

The data were collected on an ADSC Q210 CCD detector at beamline ID14-4 (λ = 0.98 Å), ESRF, Grenoble from crystals of bovine F_1-ATPase that had been conditioned at 90% relative humidity in an FMS and then cryocooled. Values in parentheses are for the highest resolution bin.

Crystal	X1	X2
Space group	$P2_12_12_1$	$P2_12_12_1$
Unit-cell parameters (Å)	a = 261.3, b = 105.3, c = 122.6	a = 262.0, b = 105.3, c = 122.9
Resolution range (Å)	20.0–1.95 (2.06–1.95)	20.0–1.96 (2.07–1.96)
No. of unique reflections	242123	219926
Multiplicity	3.5 (3.1)	3.0 (2.2)
Completeness (%)	98.8 (99.1)	91.2 (66.1)
$R_{\rm merge}$†	0.084 (0.53)	0.069 (0.50)
$\langle I/\sigma(I)\rangle$	9.2 (2.0)	10.9 (2.0)
Wilson B factor (Å^2)	27.3	26.3

† $R_{\rm merge} = \sum_h \sum_i |I(h) - I(h)_i| / \sum_h \sum_i I(h)_i$, where $I(h)$ is the mean weighted intensity after rejection of outliers.

recovered their order by increasing the humidity to the optimum value (generally retaining their smaller unit-cell parameters), whereas others were damaged permanently.

3.2. Crystal cryocooling and data collection

Initially, many crystals were lost when they were cryocooled by plunging the loop into liquid nitrogen. This loss was avoided either by ensuring that the loop gripped the crystal tightly or preferably by using micro-mesh loops. No difference was noted between crystals cryocooled in oil and those cryocooled in its absence. The crystals showed no decrease in diffraction quality after cryocooling and no ice rings were observed. After cryocooling, the refined unit-cell parameters for one of the two crystals used for data collection were a = 261.3, b = 105.3, c = 122.6 Å, giving a reduction of 22% in the unit-cell volume. The a and c unit-cell parameters are both significantly smaller than those observed previously without the use of the FMS (minimum values a = 267, c = 136 Å). Diffraction was observed at a synchrotron source to a maximum resolution of 1.8 Å (Fig. 3), although the images were processed to only 1.95 Å (Table 1) as the diffraction limit dropped during data collection owing to radiation damage. A second crystal dehydrated in the same way gave a data set of very similar quality (Table 1). The reduction in the unit-cell

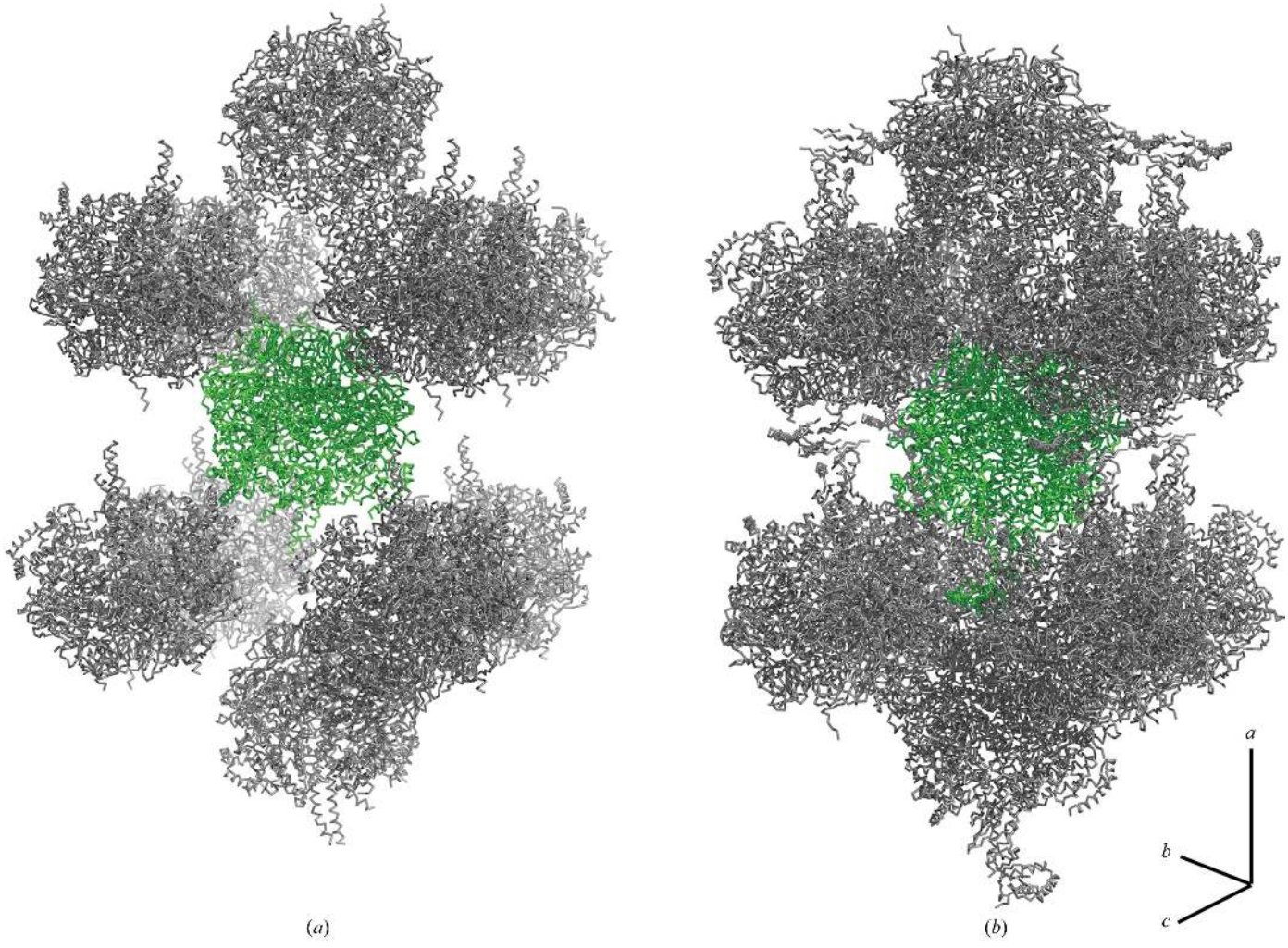

Figure 4
Crystal packing in native and dehydrated crystals of F_1-ATPase. (*a*) Native (PDB code 1e1q; Braig *et al.*, 2000); (*b*) dehydrated (PDB code 2ck3; Bowler *et al.*, 2006). The asymmetric unit is shown as a green C^α trace and symmetry-related molecules are grey. Large decreases in the a and c parameters lead to much tighter packing of the complexes and increased order of the crystal lattice.

volume leads to tighter packing and consequently to a large increase in the number of crystal contacts between complexes (Fig. 4), which presumably results in increased order within the crystal lattice.

4. Conclusions

The FMS provides a means of controlling the dehydration of crystals of F_1-ATPase and of improving their diffraction properties reproducibly below 2 Å resolution. The improved crystals were cryocooled directly in liquid nitrogen without damaging their diffraction properties. Although shrunken unit cells (with improved diffraction) have been observed previously, all previous attempts to obtain improved crystals reproducibly were unsuccessful and typically 50–75 crystals have had to be screened in order to find one with good diffraction properties (better than 2.5 Å). Many crystals exhibited poor diffraction with multiply split spots as a result of damage induced by the cryoprotection protocol [adding glycerol to a final concentration of 20%(*v*/*v*) in 5% steps]. Use of the FMS avoids the need for cryoprotection and the success rate for obtaining well ordered strongly diffracting crystals increases to approximately 75%, a dramatic improvement. Using the improved crystals of bovine mitochondrial F_1-ATPase it should be possible to increase the accuracy of the various structures of the enzyme and thus gain deeper insights into its catalytic mechanism and into the modes of action of various inhibitors.

We thank the beamline staff at the European Synchrotron Radiation Facility, Grenoble, France for assistance with data collection.

References

Abrahams, J. P., Leslie, A. G. W., Lutter, R. & Walker, J. E. (1994). *Nature (London)*, **370**, 621–628.
Bowler, M. W., Montgomery, M. G., Leslie, A. G. W. & Walker, J. E. (2006). *Proc. Natl Acad. Sci. USA*, **103**, 8646–8649.
Braig, K., Menz, R. I., Montgomery, M. G., Leslie, A. G. W. & Walker, J. E. (2000). *Structure*, **8**, 567–573.
Cramer, P., Bushnell, D. A., Fu, J., Gnatt, A. L., Maier-Davis, B., Thompson, N. E., Burgess, R. R., Edwards, A. M., David, P. R. & Kornberg, R. D. (2000). *Science*, **288**, 640–649.
Dobbek, H., Gremer, L., Meyer, O. & Huber, R. (1999). *Proc. Natl Acad. Sci. USA*, **96**, 8884–8889.
Engel, M., Hoffmann, T., Wagner, L., Wermann, M., Heiser, U., Kiefersauer, R., Huber, R., Bode, W., Demuth, H. U. & Brandstetter, H. (2003). *Proc. Natl Acad. Sci. USA*, **100**, 5063–5068.
Esnouf, R. M., Ren, J., Garman, E. F., Somers, D. O., Ross, C. K., Jones, E. Y., Stammers, D. K. & Stuart, D. I. (1998). *Acta Cryst.* D**54**, 938–953.
Estebanez-Perpina, E., Fuentes-Prior, P., Belorgey, D., Braun, M., Kiefersauer, R., Maskos, K., Huber, R., Rubin, H. & Bode, W. (2000). *Biol. Chem.* **381**, 1203–1214.
Gibbons, C., Montgomery, M. G., Leslie, A. G. W. & Walker, J. E. (2000). *Nature Struct. Biol.* **7**, 1055–1061.
Henrich, S., Cameron, A., Bourenkov, G. P., Kiefersauer, R., Huber, R., Lindberg, I., Bode, W. & Than, M. E. (2003). *Nature Struct. Biol.* **10**, 520–526.
Heras, B., Edeling, M. A., Byriel, K. A., Jones, A., Raina, S. & Martin, J. L. (2003). *Structure*, **11**, 139–145.
Kagawa, R., Montgomery, M. G., Braig, K., Leslie, A. G. W. & Walker, J. E. (2004). *EMBO J.* **23**, 2734–2744.
Kiefersauer, R., Stetefeld, J., Gomis-Ruth, F. X., Romao, M. J., Lottspeich, F. & Huber, R. (1996). *J. Appl. Cryst.* **29**, 311–317.
Kiefersauer, R., Than, M. E., Dobbek, H., Gremer, L., Melero, M., Strobl, S., Dias, J. M., Soulimane, T. & Huber, R. (2000). *J. Appl. Cryst.* **33**, 1223–1230.
Koch, M., Breithaupt, C., Kiefersauer, R., Freigang, J., Huber, R. & Messerschmidt, A. (2004). *EMBO J.* **23**, 1720–1728.
Kuo, A., Bowler, M. W., Zimmer, J., Antcliff, J. F. & Doyle, D. A. (2003). *J. Struct. Biol.* **141**, 97–102.
Kyrieleis, O. J., Goettig, P., Kiefersauer, R., Huber, R. & Brandstetter, H. (2005). *J. Mol. Biol.* **349**, 787–800.
Leslie, A. G. W. (1992). *Jnt CCP4/ESF–EACBM Newsl. Protein Crystallogr.* **26**.
Lutter, R., Abrahams, J. P., van Raaij, M. J., Todd, R. J., Lundqvist, T., Buchanan, S. K., Leslie, A. G. W. & Walker, J. E. (1993). *J. Mol. Biol.* **229**, 787–790.
Menz, R. I., Walker, J. E. & Leslie, A. G. W. (2001). *Cell*, **106**, 331–341.
Orriss, G. L., Leslie, A. G. W., Braig, K. & Walker, J. E. (1998). *Structure*, **6**, 831–837.
Raaij, M. J. van, Abrahams, J. P., Leslie, A. G. W. & Walker, J. E. (1996). *Proc. Natl Acad. Sci. USA*, **93**, 6913–6917.
Walker, J. E. (1998). *Angew. Chem. Int. Ed.* **37**, 2309–2319.